

## Hydrogen Bonding

International Edition: DOI: 10.1002/anie.201511171  
German Edition: DOI: 10.1002/ange.201511171

## Dithienophosphole-Based Phosphinamides with Intriguing Self-Assembly Behavior

Zisu Wang, Benjamin S. Gelfand, and Thomas Baumgartner\*

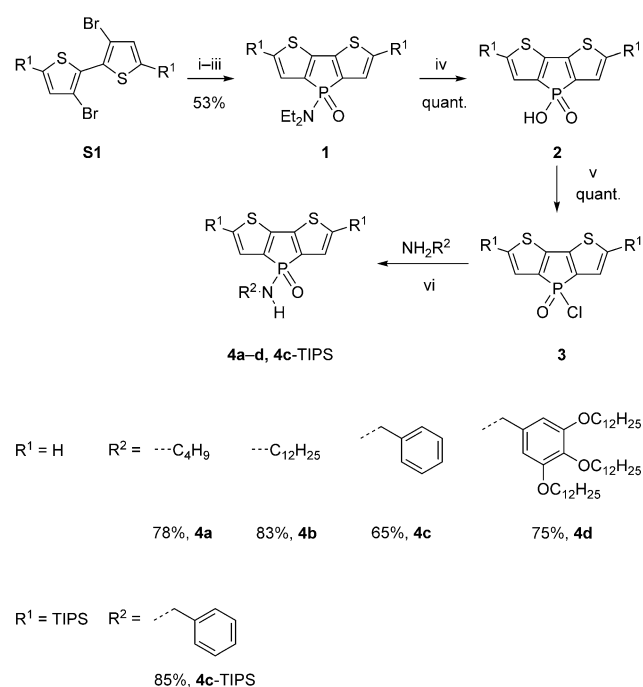
**Abstract:** A new, highly adaptable type of phosphinamide-based hydrogen bonding is representatively demonstrated in  $\pi$ -conjugated phosphole materials. The rotational flexibility of these intermolecular  $P=O-H-N$  hydrogen bonds is demonstrated by X-ray crystallography and variable-concentration NMR spectroscopy. In addition to crystalline compounds, phosphinamide hydrogen bonding was successfully introduced into the self-assembly of soft crystals, liquid crystals, and organogels, thus highlighting the high general value of this type of interaction for the formation of organic soft materials.

Organo-main-group compounds, that is, organic species exhibiting B, Si, P, Se, or Te atoms in their scaffold, have recently experienced a surge in growth as potential building blocks for electronic materials.<sup>[1]</sup> Phospholes, in particular, possess unique electronic and structural features that have made them a particularly intriguing research focus.<sup>[1a-d]</sup> In this context, we introduced self-assembled ionic phosphole lipids in 2011.<sup>[2]</sup> These amphiphilic materials display unique optoelectronic and mechanical features, and their self-assembly is governed by a fine balance of intermolecular ionic, van der Waals, and  $\pi$ -stacking interactions.<sup>[3]</sup> To further develop the supramolecular self-assembly toolbox of phosphole-based building blocks, it would be desirable to expand the interaction portfolio to include intermolecular hydrogen bonding. Hydrogen bonding plays an important role in diverse fields ranging from biochemistry to materials science. Hydrogen bonding of primary and secondary amides, in particular, is a versatile motif that can be found in various natural or synthetic materials. For example, it is crucial for the formation of secondary structures of peptides, such as  $\alpha$ -helix or  $\beta$ -sheet structures, but also for the superior strength of functional materials such as Kevlar.<sup>[4]</sup>

Phosphinamides have received some attention as a hydrogen-bonding motif;<sup>[5]</sup> the incorporation of the "PONH" building block was shown to induce unique effects on the

self-assembly of such systems. Herein, we demonstrate the synthetic value and self-assembly validity of the phosphinamide functional group with our  $\pi$ -conjugated phosphole system to develop new soft functional materials.

The new phosphinamide species was synthesized by the postfunctionalization of chlorophosphole **3**, which is accessible by a three-step protocol from the dibromobithiophene precursor **S1** (Scheme 1). By closing the phosphole ring with



**Scheme 1.** Synthesis of the phosphinamides. i)  $n$ BuLi,  $\text{Et}_2\text{O}$ ,  $-78^\circ\text{C}$ ; ii)  $\text{Et}_2\text{PCL}_2$ ,  $\text{Et}_2\text{O}$ ,  $0^\circ\text{C}$ ; reflux; iii)  $\text{H}_2\text{O}_2$ , dichloromethane, room temperature; iv) aqueous HCl, room temperature; v)  $\text{SOCl}_2$ , DMF, dichloromethane, room temperature; vi)  $\text{Et}_2\text{O}$ , room temperature. DMF = *N,N*-dimethylformamide.

an amino(dichloro)phosphane, we obtained phosphole species **1**, which can readily be further functionalized. Cleavage of the P–N bond in an aqueous medium provided us with phosphinic acid **2**. From this acid precursor, **3** was obtained by chlorination with thionyl chloride. Treatment of **3** with a series of primary alkyl amines finally afforded the corresponding phosphinamides **4a–d** and trisopropylsilyl (TIPS)-decorated **4c-TIPS** in good yields (Scheme 1).

Since dithienophospholes are commonly strongly emissive, the photophysical properties of the newly synthesized phosphinamides **1**, **4a–d**, and **4c-TIPS** were tested both in

[\*] Z. Wang, B. S. Gelfand, Prof. Dr. T. Baumgartner  
Department of Chemistry and Centre for Advanced Solar Materials  
University of Calgary  
2500 University Drive NW, Calgary, AB T2N 1N4 (Canada)  
E-mail: thomas.baumgartner@ucalgary.ca  
Homepage: <http://www.ucalgary.ca/chem/pages/Baumgartner>

Supporting information and ORCID(s) from the author(s) for this article are available on the WWW under <http://dx.doi.org/10.1002/anie.201511171>.

© 2016 The Authors. Published by Wiley-VCH Verlag GmbH & Co. KGaA. This is an open access article under the terms of the Creative Commons Attribution Non-Commercial License, which permits use, distribution and reproduction in any medium, provided the original work is properly cited, and is not used for commercial purposes.

**Table 1:** Photophysical data of the new phosphinamides.

Compound	$\lambda_{\text{abs}}$ [nm] <sup>[a]</sup>	$\log \epsilon$ <sup>[b]</sup>	$\lambda_{\text{em solution}}$ [nm] <sup>[c]</sup>	$\varphi_{\text{PL solution}}$ [%] <sup>[d]</sup>	$\lambda_{\text{em solid}}$ [nm]	$\varphi_{\text{PL solid}}$ [%] <sup>[e]</sup>
<b>1</b>	358	3.77	447	45	462	27
<b>4a</b>	355	3.77	448	57	439	22
<b>4b</b>	356	3.83	448	61	431	13
<b>4c</b>	357	3.77	450	62	445	10
<b>4d</b>	357	3.78	450	58	444 (435) <sup>[f]</sup>	11 (19) <sup>[f]</sup>
<b>4c-TIPS</b>	372	4.04	458	63	469	49

[a] The absorption wavelength was measured for a solution in dichloromethane ( $c = 1.0^{-5}$  M). [b]  $\epsilon$  is the molar absorption coefficient [ $\text{M}^{-1} \text{cm}^{-1}$ ]. [c] The emission wavelength was measured for a solution in dichloromethane ( $c = 1.0^{-5}$  M). [d] Relative photoluminescence efficiency, measured against a quinine sulfate standard adjusted to the same absorbance,  $\lambda_{\text{ex}} = 365$  nm. [e] Absolute photoluminescence efficiency, determined by the use of an integrating sphere,  $\lambda_{\text{ex}} = 365$  nm. [f] Value for the organogel of **4d** formed from *n*-heptane (8.7 mm).

solution and in their aggregated state (Table 1). The absorption spectra of the phosphinamides **4a–d** in solution are similar in terms of both wavelength (355–358 nm) and the extinction coefficient ( $3.77 \leq \log \epsilon \leq 3.83$ ), whereby the latter is roughly a quarter of the value for the parent *P*-phenyl dithienophosphole ( $\log \epsilon = 4.33$ ; 338 nm).<sup>[6]</sup> DFT calculations at the B3LYP/6-31 + G(d) level of theory<sup>[7]</sup> revealed that this relationship was due to the residence of both the HOMO and LUMO on the phosphole backbone of the compounds, in complete agreement with the frontier orbitals of the *P*-phenyl relative.

The solid-state emission spectra revealed that **4a–d** each experience a hypsochromic shift upon going from the solution to the solid state (**4a**:  $\Delta\lambda = 9$  nm, **4b**:  $\Delta\lambda = 17$  nm, **4c**:  $\Delta\lambda = 5$  nm, **4d**:  $\Delta\lambda = 6$  nm for the solid; 15 nm for the gel) that can be attributed to the formation of H-aggregates.<sup>[8]</sup> This observation, which is unprecedented for dithienophosphole-based materials, provides a basis for the discussion of the molecular ordering in the mesogenic species (see below). By contrast, neither **1** nor **4c-TIPS** showed any signs of H-aggregation (Table 1).

We used single-crystal X-ray crystallography to confirm the presence of hydrogen bonding in the new phosphole-based phosphinamide system. Suitable single crystals of **1**, **4a**, **4c**, and **4c-TIPS** were obtained by slow evaporation of the solvent (dichloromethane/hexane) at room temperature. Compound **1** was chosen as a reference control, as it does not possess any NH hydrogen atoms. As expected, limited directional anisotropy was detected in the crystal packing of **1** (Figure 1). By contrast, **4a** and **4c** both showed intermolecular hydrogen bonding between the PO acceptor and the NH donor (Figures 2 and 3). In **4a**, the combination of  $\pi$ -stacking and H-bonding causes the molecules to pack in a 1D columnar fashion. One key feature of this particular packing motif is in the head-to-tail fashion in which the molecules are assembled. Remarkably, in all previously studied non-hydrogen-bonded phospholes, for which  $\pi$ -stacking dominates, the molecules are assembled in a face-to-face pattern, in which the  $\pi$  moieties align antiparallel to each other.<sup>[9]</sup> By contrast, the  $\pi$  moieties align parallel (i.e., in a *syn*-type fashion) in the new hydrogen-bonded system; this feature was also found in **4c**. However, as can be seen in Figure 3, the H-bonding in **4c** follows a zigzag pathway (dihedral angle PO–NH: 47°;

Figure 4) instead of the nearly linear column found in **4a** (dihedral angle PO–NH: 131°; Figure 4). The deviation from the linear assembly motif in **4c** showcases an intriguing, novel structural feature of the hydrogen-bonded species: rotational flexibility of the phosphinamide bond. In classic “organic” amide H-bonding, the dihedral angle between the carbonyl group and the N–H moieties is generally found to be locked at either 0 or 180°.<sup>[4a]</sup> The conjugation that exists between the carbonyl  $\pi$  orbital and nitrogen lone pair constitutes an energetic barrier for the rotation about the C–N  $\sigma$ -bond, thus resulting in a rigidified assembly.<sup>[10]</sup> In the phosphinamide

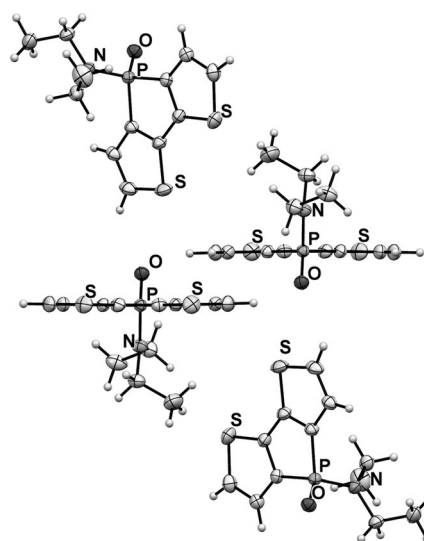


**Figure 1.** Crystallographic packing of **1**. Note the antiparallel alignment of the conjugated phosphole backbone.

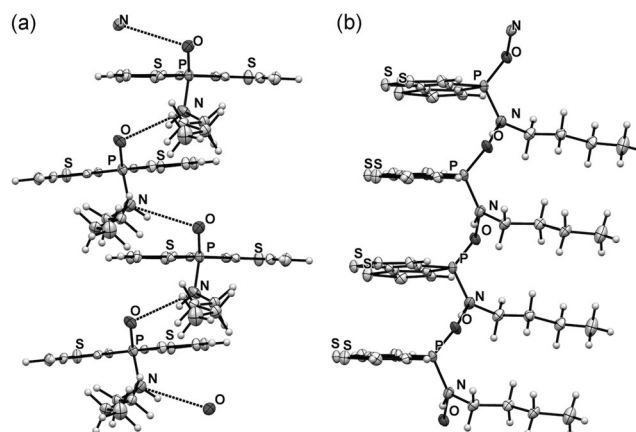


**Figure 2.** Crystallographic packing of **4a**. Intermolecular N...O distance: 2.9 Å. Note the parallel alignment of the conjugated phosphole backbone. a) Hydrogen-bonded column viewed along the butyl chain; b) hydrogen-bonded column viewed from the side.

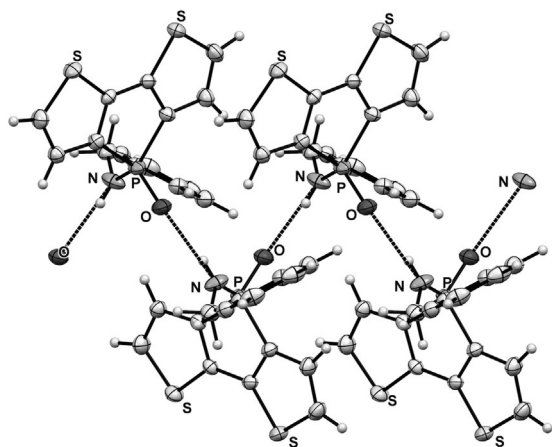


**Figure 3.** Crystallographic packing of **4c**. Intermolecular N...O distance: 2.8 Å. Note the zigzag pattern of the hydrogen bonding.

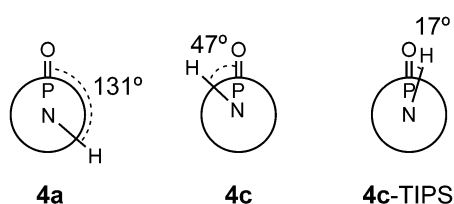


**Figure 4.** Dihedral angles between the P=O and N-H moieties in **4a**, **4c**, and **4c-TIPS**, as based on the X-ray crystallographic data.

system, owing to the distinctive bonding pattern of the tetracoordinated P center, this conjugation is considerably impeded. What results is the greater rotational freedom about the P–N bond and thus flexible hydrogen bonding.

Importantly, however, supramolecular  $\pi$ -stacking is also present in the solid-state structures of both **4a** and **4c**. The cooperative effects of the H-bonding and the  $\pi$ -stacking in these compounds ultimately lead to the formation of the linear “head-to-tail” assembly in the solid state. However, one question remains: What if the  $\pi$ -stacking were suppressed and the self-assembly process solely governed by H-bonding? To answer this question, we designed compound **4c-TIPS**. With the bulky TIPS group appended to the periphery of the backbone, the potential for  $\pi$ -stacking is removed. X-ray crystallography of **4c-TIPS** revealed that instead of ordering in a linear fashion, **4c-TIPS** adopts an edge-on motif in the solid state, with the only intermolecular interactions of note being H-bonding (Figure 5); the resulting H-bonded “head-to-head” dimer has similar bond angles to those of its organic carboxamide cousins (dihedral angle PO-NH: 17°; Figure 4, **4c-TIPS**).

Although X-ray crystallography offers useful insight into the nature of the H-bonding in a static manner, the flexible nature of the newly synthesized phosphinamides compelled us to also study the unprecedented H-bonding in a dynamic manner, that is, in solution. For this purpose, **4c** was representatively chosen for its intermediary dihedral H-bonding angle; variable-concentration (VC) NMR experi-

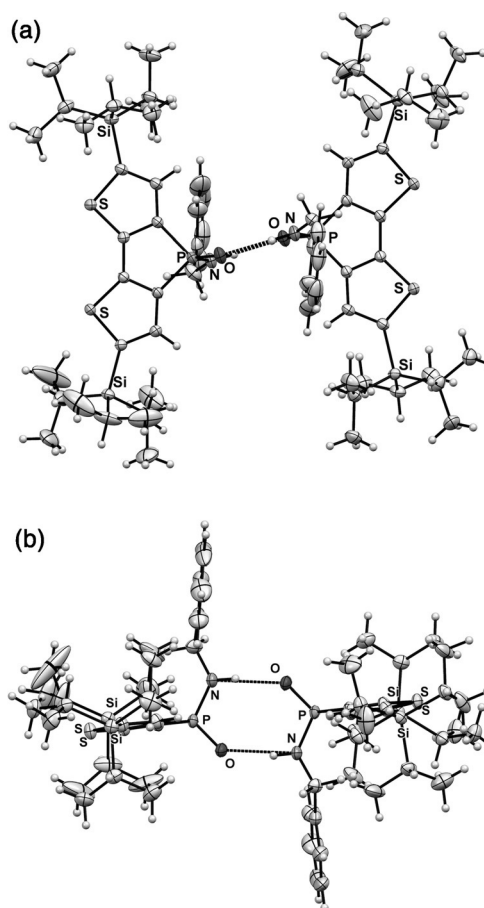


**Figure 5.** Crystallographic packing of **4c-TIPS**. Intermolecular N...O distance: 2.8 Å. a) Hydrogen-bonded dimer viewed from the top; b) hydrogen-bonded dimer viewed from the side.

**Table 2:** Dimerization constants for amides and phosphinamides.<sup>[10,11]</sup>

Compound	$K$ [ $M^{-1}$ ] <sup>[a]</sup>
$\epsilon$ -caprolactam <sup>[b]</sup>	1.4–1.8
Haley phosphaquinolone <sup>[c]</sup>	130
<b>4c</b> <sup>[c]</sup>	0.8

[a] Dimerization constant. [b] Measured for a solution in  $CHCl_3$ .

[c] Measured for a solution in  $CDCl_3$ .

ments were performed in  $CDCl_3$ . The results were fitted by the use of a program developed by Thordarson (see the Supporting Information).<sup>[11]</sup> The dimerization constant of **4c** was determined to be  $0.8 M^{-1}$ . This value is close in magnitude to the dimerization constant of *cis* amides<sup>[12]</sup> and approximately two orders of magnitudes lower than the value reported for a related cyclic phosphaquinolone by Haley and co-workers<sup>[13]</sup> (Table 2). As the Haley dimer was restricted in the *cis* conformation, the lower dimerization constant in our phosphinamide species can be attributed to the rotational flexibility of the P–N bond. Our X-ray crystallographic and NMR spectroscopic results indicate significant rotational flexibility of the P–N bond in phosphinamides **4a,c** and **4c-TIPS** in H-bond formation. Such flexi-

bility is unknown for classic amide H-bonds, such as those commonly found in peptides.

To capitalize on this unique driving force for self-assembly in the soft-materials realm, the mesogenic versions **4b,d** of the corresponding crystalline compounds **4a,c** were synthesized by treating chlorophosphole **3** with amines that were appropriately functionalized with long disorder-inducing alkyl chains. Monoalkylated **4b** exhibits soft-crystalline features at elevated temperatures, as determined by polarized optical microscopy (POM), differential scanning calorimetry (DSC), and powder X-ray diffraction (PXRD). Although crystalline features were preserved in **4b**, all attempts to grow single crystals were unsuccessful. However, on the basis of the POM patterns and the formation of H-aggregates in both **4a** and **4b**, it is inherently plausible that **4b** self-assembles into a smectic mesophase, similar to the structure of **4a** in the single crystal (Figure 6a). Owing to the presence of multiple extended alkyl

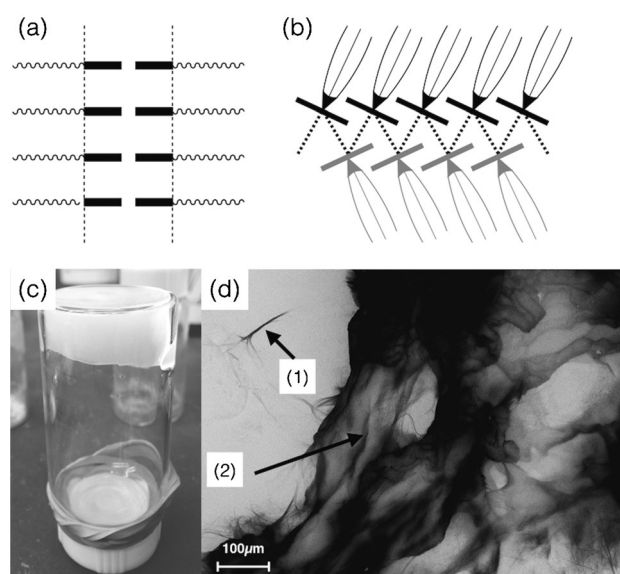


**Figure 6.** a) Proposed mesogen ordering of **4b** in the solid state; b) proposed mesogen ordering of **4d** in the solid state; c) organogel of **4d** formed from *n*-heptane; d) xerogel of **4d** under SEM; note the fiber bundle (1) and the sheetlike microstructures (2).

chains, the mesophase behavior of **4d** tends to be more on the “softer” liquid-crystalline (LC) side. Correspondingly increased disorder was observed by POM (more uniform domain features), DSC (broader thermal transitions), and PXRD (broad “humps” instead of sharp peaks; see the Supporting Information). Similar to **4b**, the combined observation of H-aggregates and the POM pattern lead us to also propose a smectic assembly pattern for **4d** (Figure 6b). More rigorous studies toward the detailed supramolecular organization of the mesophases for both **4b** and **4d** are currently under way.

Besides the observed LC self-assembly, **4d** was also able form an organogel with *n*-heptane at low concentrations (Figure 6c). Fluorescence emission spectra were collected from the gel (Table 1), and H-aggregation was also observed.

The presence of H-bonding in the organogel was moreover confirmed by IR spectroscopy and further indirectly asserted by the complete dissolution of the gel upon the addition of a small amount of methanol as a H-bond donor (see the Supporting Information). The morphology of the xerogel was studied by scanning electron microscopy (SEM), and both fiber bundles and sheetlike microstructures were observed (Figure 6d).

In conclusion, we have synthesized a new class of phosphole-containing conjugated phosphinamide compounds via the synthetically valuable chlorophosphole **3**. Single-crystal X-ray crystallography and VC NMR spectroscopy demonstrated the capacity for a new type of rotationally flexible hydrogen bonding of the compounds in both the crystalline state and solution. Mesogenic versions of the crystalline compounds were found to display soft-crystal or liquid-crystal properties at elevated temperatures as a proof of concept. Compound **4d** was also shown to form an organogel with hydrogen-bonding components. Furthermore, several of the new phosphinamides studied formed H-aggregates as a result of the unique H-bonding-directed self-assembly, thus demonstrating the considerable and general value of this structural element for the development of self-assembled soft materials. Detailed studies to expand the scope of this intriguing new supramolecular interaction are currently under way in our laboratory.

## Acknowledgments

We thank S. Mulmi and Dr. C. Reus for their assistance in collecting PXRD and SEM data, and C. Vonnegut for helpful discussions with regard to the VC NMR studies. Financial support by the NSERC of Canada and the Canada Foundation for Innovation (CFI) is gratefully acknowledged. We also thank Alberta Innovates—Technology Futures for graduate scholarships (Z.W. and B.S.G.).

**Keywords:** hydrogen bonds · phosphinamides · phosphorus heterocycles · self-assembly · soft materials

**How to cite:** *Angew. Chem. Int. Ed.* **2016**, *55*, 3481–3485  
*Angew. Chem.* **2016**, *128*, 3542–3546

- [1] a) T. Baumgartner, R. Réau, *Chem. Rev.* **2006**, *106*, 4681–4727; b) T. Baumgartner, *Acc. Chem. Res.* **2014**, *47*, 1613–1622; c) C. Romero-Nieto, T. Baumgartner, *Synlett* **2013**, *24*, 920–937; d) M. Stolar, T. Baumgartner, *Chem. Asian J.* **2014**, *9*, 1212–1225; e) F. Jäkle, *Chem. Rev.* **2010**, *110*, 3985–4022; f) S. Yamaguchi, K. Tamao in *The Organic Silicon Compounds*, Vol. 3. (Eds.: Z. Rappoport, Y. Apeloig), Wiley, Chichester, **2001**, pp. 641–694; g) J. Hollinger, D. Gao, D. S. Seferos, *Isr. J. Chem.* **2014**, *54*, 440–453; h) A. A. Jahnke, D. S. Seferos, *Macromol. Rapid Commun.* **2011**, *32*, 943–951; i) E. I. Carrera, D. S. Seferos, *Macromolecules* **2015**, *48*, 297–308.
- [2] a) Y. Ren, W. H. Kan, M. A. Henderson, P. G. Bomben, C. P. Berlinguette, V. Thangadurai, T. Baumgartner, *J. Am. Chem. Soc.* **2011**, *133*, 17014–17026; b) Y. Ren, W. H. Kan, V. Thangadurai, T. Baumgartner, *Angew. Chem. Int. Ed.* **2012**, *51*, 3964–3968; *Angew. Chem.* **2012**, *124*, 4031–4035.

- [3] X. He, J.-B. Lin, W. H. Kan, T. Baumgartner, *Angew. Chem. Int. Ed.* **2013**, *52*, 8990–8994; *Angew. Chem.* **2013**, *125*, 9160–9164.
- [4] a) A. Ben-Naim, *J. Phys. Chem.* **1991**, *95*, 1437–1444; b) K. Tashiro, M. Kobayashi, H. Tadokoro, *Macromolecules* **1977**, *10*, 413–420.
- [5] a) K. Katagiri, S. Komagawa, M. Uchiyama, K. Yamaguchi, I. Azumaya, *Org. Lett.* **2015**, *17*, 3650–3653; b) R. Ahmed, A. Altieri, D. M. D'Souza, D. A. Leigh, K. M. Mullen, M. Papmeyer, A. M. Z. Slawin, J. K. Y. Wong, J. D. Woollins, *J. Am. Chem. Soc.* **2011**, *133*, 12304–12310; c) S. Schlecht, S. Chitsaz, B. Neumüller, K. Dehnicke, *Z. Naturforsch. B* **1998**, *53*, 17–22.
- [6] T. Baumgartner, T. Neumann, B. Wirges, *Angew. Chem. Int. Ed.* **2004**, *43*, 6197–6201; *Angew. Chem.* **2004**, *116*, 6323–6328.
- [7] M. J. Frisch, et al., Gaussian09, revision C.01, Gaussian, Inc., Wallingford CT, **2009**.
- [8] F. C. Spano, C. Silva, *Annu. Rev. Phys. Chem.* **2014**, *65*, 477–500.
- [9] X. He, J.-B. Lin, W. H. Kan, P. Dong, S. Trudel, T. Baumgartner, *Adv. Funct. Mater.* **2014**, *24*, 897–906.
- [10] M. B. Robin, F. A. Bovey, H. Basch in *The Chemistry of Amides* (Ed.: J. Zabicky), Wiley, Chichester, **1970**, pp. 1–72.
- [11] P. Thordarson, *Chem. Soc. Rev.* **2011**, *40*, 1305–1323.
- [12] S. E. Krikorian, *J. Phys. Chem.* **1982**, *86*, 1875–1881.
- [13] C. L. Vonnegut, A. M. Shonkwiler, M. M. Khalifa, L. N. Zakharov, D. W. Johnson, M. M. Haley, *Angew. Chem. Int. Ed.* **2015**, *54*, 13318–13322; *Angew. Chem.* **2015**, *127*, 13516–13520.

Received: December 2, 2015

Published online: February 2, 2016